ADVANCED FUNCTIONAL MATERIALS
www.afm-journal.de

Dye Encapsulated Metal-Organic Framework for Warm-White LED with High Color-Rendering Index

*Yuanjing Cui, Tao Song, Jiancan Yu, Yu Yang, Zhiyu Wang, and Guodong Qian**

A strategy by encapsulating organic dyes into the pores of a luminescent metal-organic framework (MOF) is developed to achieve white-light-emitting phosphor. Both the red-light emitting dye 4-(*p*-dimethylaminostyryl)-1-methylpyridinium (DSM) and the green-light emitting dye acriflavine (AF) are encapsulated into a blue-emitting anionic MOF ZJU-28 through an ion-exchange process to yield the MOF⊃dye composite ZJU-28⊃DSM/AF. The emission color of the obtained composite can be easily modulated by simply adjusting the amount and component of dyes. With careful adjustment of the relative concentration of the dyes DSM and AF, the resulting ZJU-28⊃DSM/AF (0.02 wt% DSM, 0.06 wt% AF) exhibits a broadband white emission with ideal CIE coordinates of (0.34, 0.32), high color-rendering index value of 91, and moderate correlated color temperature value of 5327 K. Such a strategy can be easily expanded to other luminescent MOFs and dyes, thus opening a new perspective for the development of white light emitting materials.

1. Introduction

Solid-state white-light-emitting diodes (WLEDs) as the most promising illumination sources have attracted considerable attention because of high efficiency, long lifetime, energy savings, and environmental friendliness.[1–7] Although the combination of individual red, green, and blue LED chips into a lamp is easy to achieve white light emission, the disadvantages of high cost, different drive voltages, thermal properties and degradation trends of each LED chip restrict its wide application. An alternative method is to use a blue- or UV-LED chip combined with down-conversion emission of the phosphors. For example, the most common employment of a blue-emitting InGaN/GaN chip coupled with a yellow-emitting phosphor, $Y_3Al_5O_{12}:Ce^{3+}$ (YAG:Ce).[8,9] Unfortunately, the difference in degradation rate between the blue LED and yellow phosphor will cause chromatic aberration and poor white light performance after extensive use. In addition, the combination of blue and yellow light produces a cold white light that exhibits an unsatisfactory high correlated color temperature (CCT) of 7750 K and low color-rendering index (CRI) about 70–80 due to the deficiency of the red emission. In principle, an ideal white-light-emitting system requires the light source with the Commission International ed'Eclairage (CIE) coordinates (0.33; 0.33), with CCT between 2500 and 6500 K, and CRI above 80.[10,11] Therefore, it is urgent to develop novel single-phased warm white-light-emitting phosphor with high CRI value.

Metal-organic frameworks (MOFs) are a new family of organic–inorganic hybrid materials and have received tremendous attention in the past decades due to their exceptional tunability and structural diversity.[12–18] Because of the tremendous choices of metal nodes and organic ligands, the luminescence properties of MOFs can be elaborately designed and tuned. Such unique characteristics, as well as structural predictability and well-defined environments for luminophores either on the frameworks or into the pores, enable the luminescent MOFs to be very promising multifunctional materials for chemical sensors and light-emitting devices.[19–30] Recently, several white-light-emitting MOFs have been developed by codoping various lanthanide ions into the isostructural framework with appropriate concentration,[31–34] but the quantum yields are low due to the less energy transfer from the ligand to the lanthanide ions. In addition, the available luminescence wavelengths of these mixed lanthanide MOFs are almost fixed due to the limitation of types of lanthanide ion. For example, Eu^{3+} and Tb^{3+} ions are usually utilized to generate red and green emitting with the main transition wavelength about at 615 and 545 nm, respectively.

In fact, in addition to the doping of different lanthanide ions in the inorganic nodes of MOFs, the encapsulation of organic fluorescent dyes within the pores of MOFs can readily add another abundant luminescence behavior due to the emissive variety of organic dyes.[35–39] We speculate that if the organic dyes with different emitting color can be incorporated into pore spaces of luminescent MOFs to form MOF⊃dye composites, we should be able to make use of the combination of the emissions from MOFs and the dyes to realize the efficient white emission with high color quality. However, such white-light-emitting MOF⊃dye composites have not been explored before. Herein, we present a novel strategy to achieve white-light-emitting phosphor by encapsulating the cationic dyes 4-(*p*-dimethylaminostyryl)-1-methylpyridinium (DSM) and acriflavine (AF), which respectively exhibits red and green emission, into the pores of a blue-emitting anionic MOF ZJU-28 through

Dr. Y. Cui, T. Song, Dr. J. Yu, Dr. Y. Yang,
Prof. Z. Wang, Prof. G. Qian
State Key Laboratory of Silicon Materials
Cyrus Tang Center for Sensor Materials and Applications
School of Materials Science and Engineering
Zhejiang University
Hangzhou 310027, China
E-mail: gdqian@zju.edu.cn

DOI: 10.1002/adfm.201501756

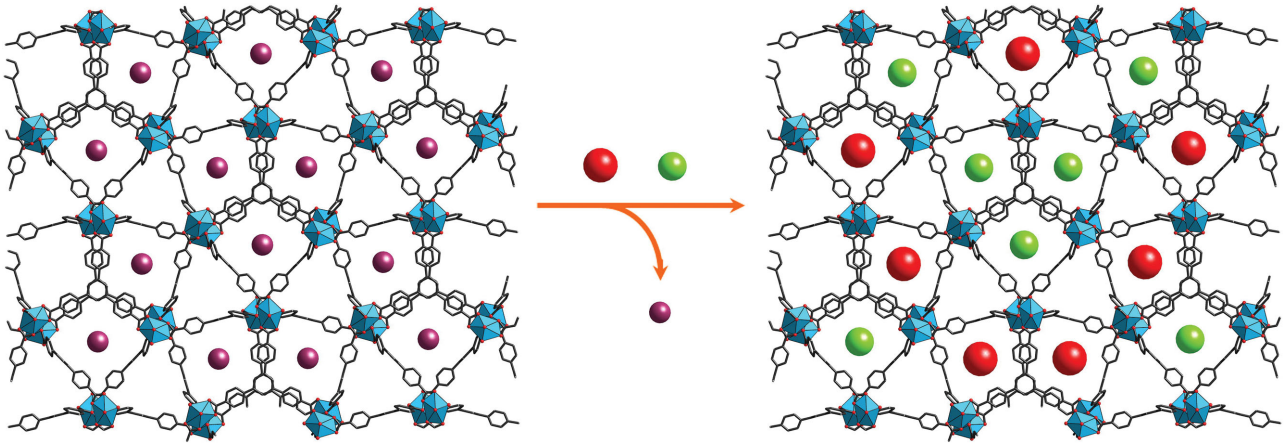

Scheme 1. Schematic illustration of the enscapulation of cationic dyes into ZJU-28 via ion-exchange process.

an ion-exchange process (**Scheme 1**). The resultant MOF⊃dye composite exhibits a high quantum yield of 17.4% because that the confinement and isolation of the MOFs efficiently restrict the aggregation-caused quenching of the dyes. Furthermore, the new composite emits a highly pure white light good color quality, as evident from the nearly ideal CIE coordinates of (0.34, 0.32), the high CRI of 91 and the appropriate CCT of 5327 K.

2. Results and Discussion

2.1. Synthesis and Structure

Micrometer-sized single crystals of anionic MOF ZJU-28 were synthesized via a solvothermal reaction of 4,4′,4″-benzene-1,3,5-triyl-tri-benzate (H_3BTB) and $InCl_3$ as described in the literature.[35] The MOF ZJU-28 is a crystalline porous material of two types of 1D channels along *c*-axis of about 6.1 × 6.1 and 7.1 × 8.5 $Å^2$, respectively (Figure S1, Supporting Information). The channels and void spaces were occupied by abundant highly disordered solvent molecules and Me_2NH_2 cations, which were estimated to be 64.7% of the total volume. Similar to the recent studies of anionic MOFs,[35,36,40–43] these endogenous Me_2NH_2 cations can undergo facile exchange with exogenous cations due to the strong electrostatic interactions, thus enabling the introduction of cationic dyes into the pores of the MOFs. Importantly, this exchange approach would not require additional chemical modification of the existing frameworks and dyes. Furthermore, it should be effective for encapsulating diverse dyes with different emission colors in the single MOF.

To encapsulate the dyes into the channel pores of ZJU-28, the as-synthesized MOF crystals were soaked in the dimethylformamide (DMF) solutions of cationic dye DSM, AF, or the mixture of DSM and AF at ambient temperature for about 8 h. Subsequently, the resulting samples were filtered off, washed several times with DMF until no characteristic emission was observed in the filtrate upon excitation, and then dried in air. The exchange reaction of Me_2NH_2 cations by different dyes was accompanied by a color change of the ZJU-28 crystals and yields the MOF⊃dye composite ZJU-28⊃DSM, ZJU-28⊃AF and ZJU-28⊃DSM/AF, respectively. The resultants were characterized by Fourier transform infrared (FTIR) spectra (Figure S6, Supporting Information) and powder X-ray diffraction (PXRD). As shown in **Figure 1**, the PXRD data for these dye-exchanged MOFs were nearly identical to those for the parent MOF ZJU-28, indicating that the cation-exchange process do not destroy the crystal structure. By varying the solution concentration from 0.001 to 0.5 mmol L^{-1}, a series of dye-exchanged MOFs ZJU-28⊃DSM, ZJU-28⊃AF and ZJU-28⊃DSM/AF with different dye content can be achieved. Furthermore, after soaking these dye-exchanged MOFs (1 mg) into DMF (10 mL) for 24 h, no obvious emission band attributed to the dye has been observed in the luminescent spectra of the filtrate (Figure S7, Supporting Information). The results indicate that the strong electrostatic interactions between cationic dyes and anionic framework of ZJU-28 could effectively limit the release of the dyes from the pores of MOFs.

2.2. Photoluminescent Properties and Tuning of Emission Colors

Upon excited at 365 nm, the crystals of ZJU-28 exhibit the blue emission with an emission maximum at 415 nm derived

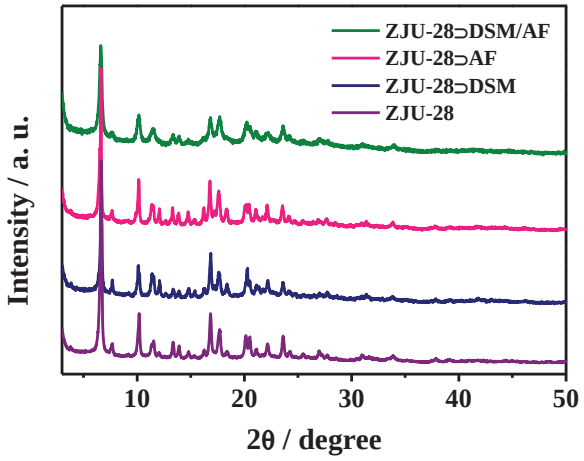

Figure 1. XRD patterns of ZJU-28, ZJU-28⊃DSM, ZJU-28⊃AF, and ZJU-28⊃DSM/AF.

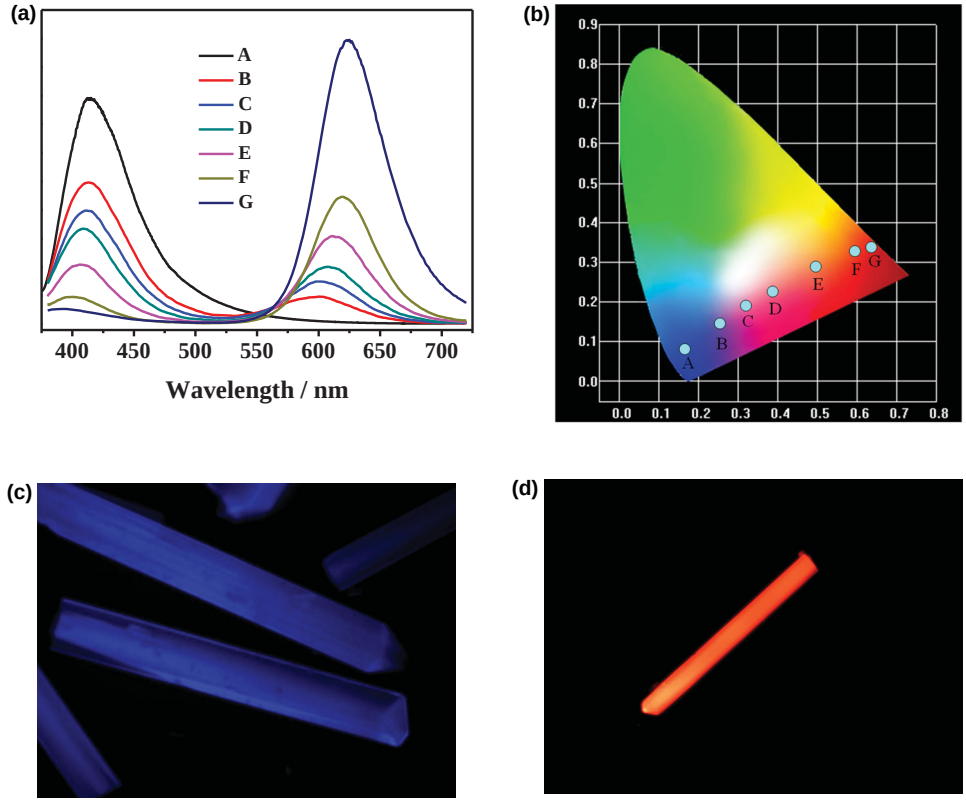

Figure 2. a) Emission spectra and b) corresponding CIE chromaticity coordinates of ZJU-28⊃DSM with different amounts of DSM (A, 0; B, 0.01 wt%; C, 0.02 wt%; D, 0.04 wt%; E, 0.09 wt%; F, 0.19 wt%; G, 0.35 wt%) excited at 365 nm. Photographs of c) ZJU-28 and d) ZJU-28⊃DSM with 0.35 wt% DSM under 365 nm UV light.

from the H_3BTB ligand (Figures S9 and S10, Supporting Information). The CIE coordinates for the emission of ZJU-28 was calculated to be (0.16, 0.08), which is closed to the saturated blue emitter with a CIE coordinates of (0.14, 0.08). The DSM solution in DMF (10^{-6} mol L^{-1}) displays strong red emission around 625 nm in the emission spectrum under a 468 nm excitation (Figure S11, Supporting Information). Due to the spectral overlap between the absorption of dye DSM and the emission of ZJU-28 (Figure S12, Supporting Information), the efficient excitation energy transfer from MOF ZJU-28 to the dye DSM may be occurred. Such a MOF-to-dye energy transfer behavior has been confirmed by the emission spectra of ZJU-28⊃DSM excited at 365 nm which belongs to the excitation wavelength of the MOF ZJU-28. As shown in **Figure 2**a, although the dye DSM has much less absorption at 365 nm, the significant emission of DSM can be observed in ZJU-28⊃DSM due to the sensitization of the MOF ZJU-28. The MOF-to-dye energy transfer makes it possible to obtain both the blue emission of the MOF ZJU-28 and the red emission of the dye DSM in a single material, which is the basis for tuning the emission color under a single excitation of UV light. As expected, the luminescent band centered at about 610 nm from the dye DSM is readily generated in addition to the original emission of the MOF ZJU-28 when the dye-exchanged MOF ZJU-28⊃DSM was excited at 365 nm (Figure 2a). This change of luminescence spectra also indicates the successful encapsulation of DSM into the pores of ZJU-28. Furthermore, the fluorescent images in different depth recorded by laser confocal scanning microscope display a uniform distribution in a single crystal, indicating that the dye DSM was dispersed throughout the MOF ZJU-28 and not just on the outside surface. In the emission spectra of ZJU-28⊃DSM with dierfferent content of DSM (Figure 2a), the blue emission band of ZJU-28 is gradually quenched when the dye concentration gradually increases from 0.01 to 0.35 wt%, with the subsequent enhancement of red emission bands attributed to the dye DSM. In addition, the emission band of DSM gradually shifted to the longer wavelength region with an increase in the amount of added DSM, which may be attributed to reabsorption effects and/or dye aggregation at higher concentrations.

Encapsulation of fluorescent dye DSM into the MOF ZJU-28 also enables flexible tuning of the emission colors within a wide range of the visible spectrum. The colors of the emissions from dye-encapsulated MOF ZJU-28⊃DSM were plotted in the CIE 1931 chromaticity diagram (Figure 2b). The emission colors of ZJU-28⊃DSM varied from blue to purple, particularly at high concentrations of the dye, exhibited the dominant color of the dye DSM as red eventually (Figure 2c,d), suggesting that emission color of the dye-exchanged MOFs can be easily tuned by controlling the required amounts of the dye DSM. The ZJU-28⊃DSM containing 0.35 wt% DSM exhibits red emission with CIE coordinates of (0.63, 0.34), closing to that of saturated red emitter with CIE coordinates of (0.66, 0.33). These results indicate that the ZJU-28⊃DSM with 0.35 wt% DSM is an efficient red-light emitter.

Table 1. Quantum yield of the DSM solution in DMF and ZJU-28⊃DSM with different dye content.

Sample	Quantum yield[%]
DSM solution (10^{-6} mol L^{-1})	6.93
DSM solution (10^{-5} mol L^{-1})	4.54
DSM solution (10^{-4} mol L^{-1})	0.11
ZJU-28⊃DSM (0.01 wt% DSM)	55.47
ZJU-28⊃DSM (0.02 wt% DSM)	60.72
ZJU-28⊃DSM (0.04 wt% DSM)	56.75
ZJU-28⊃DSM (0.19 wt% DSM)	53.75
ZJU-28⊃DSM (0.35 wt% DSM)	53.48

It is to be mentioned that the dye DSM in ZJU-28⊃DSM shows the significant enhancement in emission intensity and fluorescence quantum efficiency compared with the DSM powder or solution due to the pore confinement of MOF ZJU-28. As shown in **Table 1**, the DSM exhibits the low fluorescence quantum efficiency of 6.93% in DMF solution (10^{-6} mol L^{-1}), while exhibits very high quantum efficiency up to 60.72% in ZJU-28⊃DSM sample with a dye content of 0.02 wt%. This result demonstrates that the confinement and isolation of the DSM molecules within the pores of ZJU-28 can effectively restrain the intramolecular torsional motion and increase the conformational rigidity of the dye, thus significantly diminishes the aggregation-caused quenching and populates its radiative decay pathway. As shown in Tables S2 and S3, Supporting Information, the similar luminescent enhancement behaviors were also achieved by encapsulating DSM into the anionic MOFs NOTT-210 (NOTT-210 = In-TPTC, TPTC = terphenyl-3,3^2,5,5^2-tetracarboxylate) and bio-MOF-1 (bio-MOF-1 = $Zn_8(ad)_4(BPDC)_6O\cdot 2Me_2NH_2$, ad = adeninate, BPDC = biphenyldicarboxylate).[40–42] This further demonstrates that the confinement of dye within the MOF is effective for enhancing the fluorescence quantum efficiency.

The enhanced luminescence quantum efficiency and color tunability of ZJU-28⊃DSM inspired us to further investigate the luminescence properties of acriflavine-exchanged MOF ZJU-28⊃AF. As shown in **Figure 3**, the similar results were also realized in ZJU-28⊃AF. When the concentration of dye AF gradually increases, the green emission band peaked at about 530 nm of AF is enhanced while the blue one of ZJU-28 is gradually diminished. Thus, the emission colors of ZJU-28⊃AF changed from blue to green. In particular, the MOF ZJU-28⊃AF containing 0.21 wt% AF exhibited a green light emission with CIE coordinates of (0.28, 0.61).

2.3. Fabrication of White LED Device

Considering that the dye-exchanged MOFs ZJU-28⊃DSM and ZJU-28⊃AF are excellent red and green emitter, respectively, we explored their capability to yield white-light emission by balance the distribution of the three emissions from DSM, AF, and ZJU-28. The mixed-dye-exchanged MOFs ZJU-28⊃DSM/AF can be conveniently prepared by soaking the MOF ZJU-28 into the mixed solution of DSM and AF, and the encapsulated amount of dyes can be controlled and fine-tuned by varying immersing time and solution concentration. The optimal white-light emission was realized when the concentration of DSM and AF was adjusted to 0.02 wt% and 0.06 wt%, respectively. At this concentration, a broadband emission covering the whole visible spectral region can be achieved when excited at 365 nm (Figure 4a). The CIE chromaticity coordinates was measured as (0.34, 0.32) (Figure 4b), which is very close to those of the ideal white light (0.33, 0.33). Furthermore, the broadband emission would be beneficial to overcome the major drawback of many lanthanide phosphors, such as low CRI value. As expected, the CCT and CRI values of ZJU-28⊃DSM/AF (0.02 wt% DSM, 0.06 wt% AF) were determined to be 5327 and 91, respectively. The absolute quantum yield (QY) was measured as 17.4% by exciting the samples with diffuse light within an integrating sphere. These values are quite high as compared to the similar reported white-light-emitting MOFs.

Clearly, such a dye-exchanged MOF platform enables us to readily fabricate single-phased white-light emitting materials by modulating the amounts and components of encapsulated dyes. To assess its universality, the other cationic acridine dye 10-methyl-acridine (AcrM) was encapsulated into the MOF ZJU-28 and NOTT-210 as green-light-emitting component

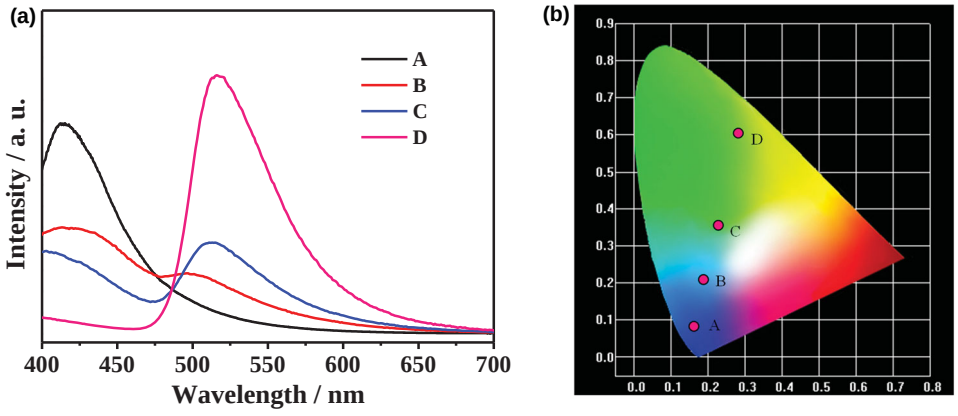

Figure 3. a) Emission spectra and b) corresponding CIE chromaticity coordinates of ZJU-28⊃AF with different contents of AF (A, 0; B, 0.01 wt%; C, 0.02 wt%; D, 0.21 wt%) excited at 365 nm.

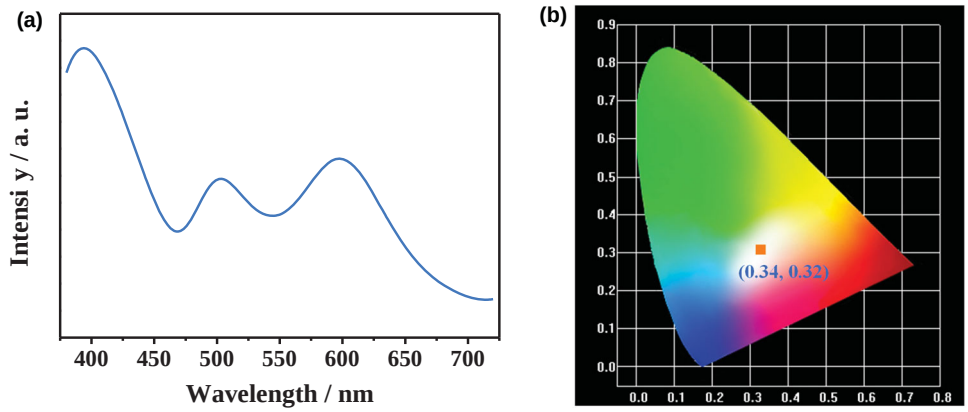

Figure 4. a) Emission spectrum and b) emission colors in the CIE 1931 chromaticity diagram of ZJU-28⊃DSM/AF (0.02 wt% DSM, 0.06 wt% AF) excited at 365 nm.

(Figures S13–S16, Supporting Information). As expect, the resultant dye-exchanged MOFs ZJU-28⊃DSM/AcrM and NOTT-210⊃DSM/AcrM under excitation of UV light also exhibit the broadband white-light emission with the CIE coordinates of (0.34, 0.32) and (0.31, 0.32), respectively (Figures S17 and S18, Supporting Information). Furthermore, the ZJU-28⊃DSM/AcrM exhibits good color quality with a corresponding CRI value of 86 and CCT value of 5004 K, respectively.

To further demonstrate the potential of dye-encapsulated MOFs for practical white-light emitting application, white-light-emitting LED device was fabricated by simply coating the ZJU-28⊃DSM/AF (0.02 wt% DSM, 0.06 wt% AF) as phosphor at the curved surface of the commercial 365 nm ultraviolet LED chip. As illustrated in **Figure 5**, the resultant LED device glowed with bright white color when the LED chip were connected to the electrical power of 3.8 V, suggesting that the dye-encapsulated MOFs are promising phosphor materials for practical lighting applications.

3. Conclusion

In summary, we have demonstrated a novel dye-encapsulated MOF strategy for the design of white-emitting phosphors with superior performance. By combining and tuning the multiple emissions from the MOFs and the dyes, a single-phased white-light-emitting phosphor with ideal CIE coordinates of (0.34, 0.32), high CRI value of 91 and moderate CCT value of 5327 K was obtained, demonstrating its promising applicability to the warm-white light-emitting diodes. The confinement of the organic fluorescence dyes within the pores of MOFs not only provided a fine tuning of emission color to attain white light, but also efficiently enhance the fluorescence quantum efficiency by blocking the aggregation-caused quenching process of the dyes. Because a variety of organic dyes with high quantum effeciency, such as coumarin, boron dipyrromethene, and rhodamine, can also be encapsulated into a large number of available luminescent MOFs to systematically tune the emission color and quality, the strategy we report here offers a great flexibility and very many options in rational design of white phosphors, thus opening a new approach to develop high-performance white light-emitting diodes.

4. Experimental Section

Synthesis of 4-[p-(dimethylamino)styryl]-1-methylpyridinium iodide: 4-Picoline (9.30 g, 0.10 mol) was dissolved in THF (200 mL), and stirred vigorously, while methylene iodide (56.70 g, 0.40 mmol, 24.9 mL) was added dropwise. The resultant mixture was refluxed for 6 h. After THF and methylene iodide were removed, brown needle-like

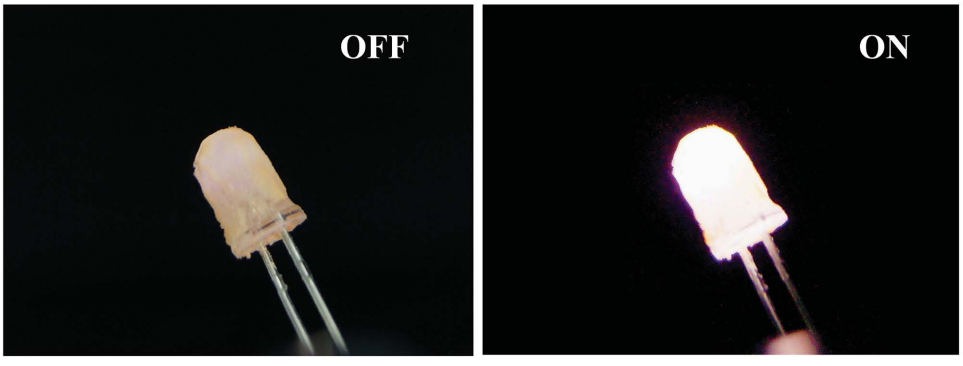

Figure 5. Photographs of the 365 nm ultraviolet LED coated with ZJU-28⊃DSM/AF (0.02 wt% DSM, 0.06 wt% AF) phosphor when the LED is tuned off and tuned on.

crystals of 1,4-dimethylpyridinium iodide were obtained and used for the following reaction without further purification. To a solution of 4-(*N*,*N*-dimethylamino)benzaldehyde (14.95 g, 100 mmol) and 1,4-dimethylpyridinium iodide (23.10 g, 98 mmol) in ethanol (250 mL) was added piperidine (2.00 mL). The yellow solution was refluxed for 1 d and then cooled to room temperature. The resultant precipitate was collected and recrystallized from methanol to yield red needle like crystals of 4-[*p*-(dimethylamino)styryl]-1-methylpyridinium iodide (DSM, 25.90 g, 72%). Mp: 262 °C. ^{1}H NMR (DMSO-d_6, δ ppm) 8.67 (d, J = 6Hz, 2H), 8.04 (d, J = 6Hz, 2H), 7.90 (d, J = 16Hz, 1H), 7.59 (d, J = 8.5Hz, 2H), 7.17 (d, J = 16Hz, 1H), 6.78 (d, J = 8.5Hz, 2H), 4.17 (s, 3H), 3.02 (s, 6H). Calcd. for $C_{16}H_{19}IN_2$ (366.24): C, 52.47; H, 5.23; N, 7.65. Found: C, 52.49; H, 5.28; N, 7.54.

Synthesis of 10-methylacridinium: Acridine (1.80 g, 0.01 mol) and methyl iodide (1.42 g, 0.03 mol) was dissolved in acetonitrile. The mixture was refluxed for 12 h, and then the solvents and methyl iodide were removed by rotary evaporator. The crude product was collected and recrystallized from ethanol and DMF to yield the dye AcrM. ^{1}H NMR (DMSO-d_6, δ ppm), 10.19 (s, 1H), 8.19 (d, J = 9.0 Hz, 2H), 8.64 (d, J = 8.5 Hz, 2H), 8.48 (t, J = 8.0 Hz, 2H), 8.04 (t, J = 9.0 Hz, 2H), 4.86 (s, 3H). Calcd. for $C_{14}H_{12}IN$ (321.16): C, 52.36; H, 3.77; N, 4.36, Found: C: 52.67; H: 3.61; N: 4.15.

Synthesis of the Anionic MOFs ZJU-28, NOTT-210, and bio-MOF-1: The synthesis of the MOFs ZJU-28, NOTT-210, and bio-MOF-1 were carried out according to a literature method.[35,40–42]

Preparation of the Dye-Encapsulated MOFs: Crystals of ZJU-28 were immersed in a DSM solution in DMF with varying concentrations from 0.001 to 0.5 mmol L^{-1} at ambient temperature for 8 h to yield a series of ZJU-28⊃DSM composites with different DSM content. The products were washed thoroughly with DMF and ethanol for several times to remove residual DSM on the surface of ZJU-28, and dried at 60 °C for 4 h. Utlizing the similar method, the composites ZJU-28⊃AF, NOTT-210⊃DSM, and bio-MOF-1⊃DSM were obtained.

Preparation of the Dye-Encapsulated MOFs ZJU-28⊃DSM/AF for LED: The dye-encapsulated MOFs ZJU-28⊃DSM/AF was prepared by immersing the crystals of ZJU-28 in the mixed solutions of DSM and AF with different molar ratios. After 4 to 24 h of soakage, the crystals were taken out of solution and washed with DMF to remove residual dyes on the surface. Utlizing the similar method, the composites ZJU-28⊃DSM/AcrM and NOTT-210⊃DSM/AcrM were obtained. The white-light-emitting LED device was fabricated by coating the as-prepared ZJU-28⊃DSM/AF (0.02 wt% DSM, 0.06 wt% AF) powders as phosphor at the curved surface of the commercial 365 nm ultraviolet LED chip.

Supporting Information

Supporting Information is available from the Wiley Online Library or from the author.

Acknowledgements

The authors gratefully acknowledge financial support from National Natural Science Foundation of China (Nos. 51272229, 51272231, 51229201, 51472217, and 51432001), Zhejiang Provincial Natural Science Foundation of China (Nos. LR13E020001 and LZ15E020001), Qianjiang Talent Project (No. QJD1302009), Fundamental Research Funds for the Central Universities (Nos. 2015QNA4009, 2015FZA4008, and 2014XZZX005), and Program for Innovative Research Team in University of Ministry of Education of China (IRT13R54).

Received: April 29, 2015
Revised: June 3, 2015
Published online: July 3, 2015

[1] L. D. Carlos, R. A. S. Ferreira, V. de Zea Bermudez, B. Julián-López, P. Escribano, *Chem. Soc. Rev.* **2011**, *40*, 536.
[2] J. Kido, M. Kimura, K. Nagai, *Science* **1995**, *267*, 1332.
[3] C. Y. Sun, X. L. Wang, X. Zhang, C. Qin, P. Li, Z. M. Su, D. X. Zhu, G. G. Shan, K. Z. Shao, H. Wu, J. Li, *Nat. Commun.* **2013**, *4*, 2717.
[4] M.-S. Wang, S.-P. Guo, Y. Li, L.-Z. Cai, J.-P. Zou, G. Xu, W.-W. Zhou, F.-K. Zheng, G.-C. Guo, *J. Am. Chem. Soc.* **2009**, *131*, 13572.
[5] Y.-C. Liao, C.-H. Lin, S.-L. Wang, *J. Am. Chem. Soc.* **2005**, *127*, 9986.
[6] J. He, M. Zeller, A. D. Hunter, Z. Xu, *J. Am. Chem. Soc.* **2012**, *134*, 1553.
[7] E. R. Dohner, A. Jaffe, L. R. Bradshaw, H. I. Karunadasa, *J. Am. Chem. Soc.* **2014**, *136*, 13154.
[8] S. P. Lee, C. H. Huang, T. S. Chan, T. M. Chen, *ACS Appl Mater Interfaces* **2014**, *6*, 7260.
[9] Y. C. Wu, D. Y. Wang, T. M. Chen, C. S. Lee, K. J. Chen, H. C. Kuo, *ACS Appl. Mater Interfaces* **2011**, *3*, 3195.
[10] S. V. Eliseeva, J.-C. G. Bunzli, *Chem. Soc. Rev.* **2010**, *39*, 189.
[11] B. W. D'Andrade, S. R. Forrest, *Adv. Mater.* **2004**, *16*, 1585.
[12] M. O'Keeffe, O. M. Yaghi, *Chem. Rev.* **2012**, *112*, 675.
[13] A. U. Czaja, N. Trukhan, U. Müller, *Chem. Soc. Rev.* **2009**, *38*, 1284.
[14] J.-R. Li, J. Sculley, H.-C. Zhou, *Chem. Rev.* **2012**, *112*, 869.
[15] P. Horcajada, R. Gref, T. Baati, P. K. Allan, G. Maurin, P. Couvreur, G. Férey, R. E. Morris, C. Serre, *Chem. Rev.* **2012**, *112*, 1232.
[16] B. Chen, S. Xiang, G. Qian, *ACC. Chem. Res.* **2010**, *43*, 1115.
[17] P. Ramaswamy, N. E. Wong, G. K. Shimizu, *Chem. Soc. Rev.* **2014**, *43*, 5913.
[18] Z. Zhang, M. J. Zaworotko, *Chem. Soc. Rev.* **2014**, *43*, 5444.
[19] M. D. Allendorf, C. A. Bauer, R. K. Bhakta, R. J. T. Houk, *Chem. Soc. Rev.* **2009**, *38*, 1330.
[20] Y. Cui, Y. Yue, G. Qian, B. Chen, *Chem. Rev.* **2012**, *112*, 1126.
[21] L. E. Kreno, K. Leong, O. K. Farha, M. Allendorf, R. P. Van Duyne, J. T. Hupp, *Chem. Rev.* **2012**, *112*, 1105.
[22] S. Furukawa, J. Reboul, S. Diring, K. Sumida, S. Kitagawa, *Chem. Soc. Rev.* **2014**, *43*, 5700.
[23] Z. Hu, B. J. Deibert, J. Li, *Chem. Soc. Rev.* **2014**, *43*, 5815.
[24] S. T. Zheng, J. J. Bu, T. Wu, C. Chou, P. Feng, X. Bu, *Angew. Chem. Int. Ed.* **2011**, *50*, 8858.
[25] H.-L. Jiang, Y. Tatsu, Z.-H. Lu, Q. Xu, *J. Am. Chem. Soc.* **2010**, *132*, 5586.
[26] Y. J. Cui, H. Xu, Y. F. Yue, Z. Y. Guo, J. C. Yu, Z. X. Chen, J. K. Gao, Y. Yang, G. D. Qian, B. L. Chen, *J. Am. Chem. Soc.* **2012**, *134*, 3979.
[27] X. T. Rao, T. Song, J. K. Gao, Y. J. Cui, Y. Yang, C. D. Wu, B. L. Chen, G. D. Qian, *J. Am. Chem. Soc.* **2013**, *135*, 15559.
[28] Y. J. Cui, W. F. Zou, R. J. Song, J. C. Yu, W. Q. Zhang, Y. Yang, G. D. Qian, *Chem. Commun.* **2014**, *50*, 719.
[29] Z. Dou, J. Yu, Y. Cui, Y. Yang, Z. Wang, D. Yang, G. Qian, *J. Am. Chem. Soc.* **2014**, *136*, 5527.
[30] J. Yu, Y. Cui, C. D. Wu, Y. Yang, B. Chen, G. Qian, *J. Am. Chem. Soc.* **2015**, *137*, 4026.
[31] Q. Tang, S. Liu, Y. Liu, D. He, J. Miao, X. Wang, Y. Ji, Z. Zheng, *Inorg. Chem.* **2013**, *53*, 289.
[32] X. Rao, Q. Huang, X. Yang, Y. Cui, Y. Yang, C. Wu, B. Chen, G. Qian, *J. Mater. Chem.* **2012**, *22*, 3210.
[33] S. Dang, J.-H. Zhang, Z.-M. Sun, *J. Mater. Chem.* **2012**, *22*, 8868.
[34] K. Liu, H. You, Y. Zheng, G. Jia, Y. Song, Y. Huang, M. Yang, J. Jia, N. Guo, H. Zhang, *J. Mater. Chem.* **2010**, *20*, 3272.
[35] J. Yu, Y. Cui, C. Wu, Y. Yang, Z. Wang, M. O'Keeffe, B. Chen, G. Qian, *Angew. Chem. Int. Ed.* **2012**, *51*, 10542.
[36] J. Yu, Y. Cui, H. Xu, Y. Yang, Z. Wang, B. Chen, G. Qian, *Nat. Commun.* **2013**, *4*, 2719.

[37] M. J. Dong, M. Zhao, S. Ou, C. Zou, C. D. Wu, *Angew. Chem. Int. Ed.* **2014**, *53*, 1575.
[38] R. Grunker, V. Bon, A. Heerwig, N. Klein, P. Muller, U. Stoeck, I. A. Baburin, U. Mueller, I. Senkovska, S. Kaskel, *Chemistry* **2012**, *18*, 13299.
[39] Q.-R. Fang, G.-S. Zhu, Z. Jin, Y.-Y. Ji, J.-W. Ye, M. Xue, H. Yang, Y. Wang, S.-L. Qiu, *Angew. Chem. Int. Ed.* **2007**, *46*, 6638.
[40] S. Yang, S. K. Callear, A. J. Ramirez-Cuesta, W. I. F. David, J. Sun, A. J. Blake, N. R. Champness, M. Schröder, *Faraday Discuss.* **2011**, *151*, 19.
[41] J. An, S. J. Geib, N. L. Rosi, *J. Am. Chem. Soc.* **2009**, *131*, 8376.
[42] J. An, C. M. Shade, D. A. Chengelis-Czegan, S. Petoud, N. L. Rosi, *J. Am. Chem. Soc.* **2011**, *133*, 1220.
[43] D. T. Genna, A. G. Wong-Foy, A. J. Matzger, M. S. Sanford, *J. Am. Chem. Soc.* **2013**, *135*, 10586.